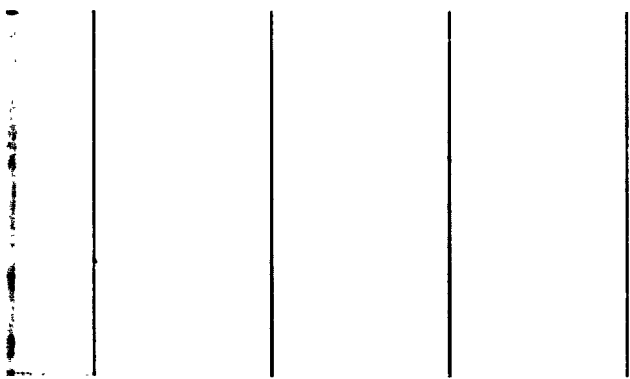


UNITED STATES
DEPARTMENT OF THE INTERIOR
BUREAU OF MINES



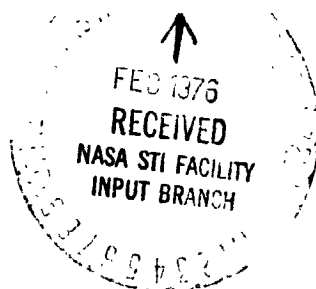
(NASA-CF-146359) SURFACE FRICTION OF ROCK
IN TERRESTRIAL AND SIMULATED LUNAR
ENVIRONMENTS (Bureau of Mines) 35 p HC
\$4.00

N76-17250

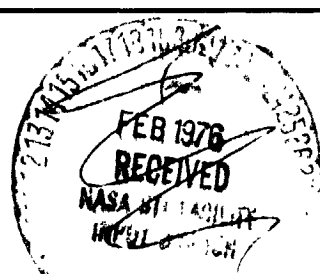
CSCL 11G

G3/27

Unclas
14608



TWIN CITIES MINING RESEARCH CENTER



U.S. Department of the Interior
Bureau of Mines

Contract Report for Contract No. R-09-040-001
Monitored by Mr. James Gangler
NASA - OART

**SURFACE FRICTION OF ROCK IN TERRESTRIAL
AND SIMULATED LUNAR ENVIRONMENTS**

by

Wallace W. Roepke and Syd S. Peng
Twin Cities Mining Research Center
Minneapolis, Minnesota

April 1975

SURFACE FRICTION OF ROCK IN TERRESTRIAL
AND SIMULATED LUNAR ENVIRONMENTS

by

Wallace W. Roepke¹ and Syd S. Peng²

ABSTRACT

The conventional probe-on-the-rotating-disk concept was used to determine the surface friction in mineral probe/specimen interfaces. Nine rocks or minerals and two stainless steels were tested in both new (NT) and same track (ST) tests under three different pressure environments (atmospheric, UHV, and dry nitrogen). Each environment was further subdivided into two testing conditions, that is, ambient and elevated (135° C) temperatures. In NT tests, friction was the lowest in an atmospheric pressure condition for all rock types and increased to the largest in UHV ambient condition except for pyroxene and stainless steel. Friction values measured in dry nitrogen ambient condition lie between the two extremes. Heating tends to increase friction in atmospheric and dry nitrogen environment but decrease in UHV environment with the exception of stainless steel, basalt, and pyroxene. In ST tests, friction was the lowest in the first run and increased in subsequent runs except for stainless steel where the reverse was true. The increases leveled off after a few runs ranging from the second to the seventh depending on rock types. The effects of environments on the friction in ST tests followed those in NT tests. Possible mechanisms of these changes in frictional values are presented based on

¹Principal vacuum specialist

²Mining engineer. (Now with School of Mines, West Virginia University, Morgantown, W. Va.)

the frictional traces, surface profiles of the specimens before and after the tests, and videotaped macroscopic inspection of some tests. The characteristics of the frictional traces favor junction adhesion theory of friction. Several recommendations for further study are made based on this initial research work.

INTRODUCTION

The U.S. Bureau of Mines studied problems associated with handling in situ materials on the lunar surface under a contract funded by NASA's Office of Advanced Research and Technology.³ The objectives of these

³This work was performed under NASA contract No. R-09-040-001 monitored by Mr. J. J. Gangler from the Office of Advanced Research and Technology.

studies were to provide support for future manned space missions by supplying basic scientific and engineering information concerning the use of extraterrestrial mineral resources and materials handling characteristics. These studies were carried on as a series of coordinated research projects at several Bureau Research Centers.

Friction tests of simulated lunar materials at the simulated lunar vacuum were performed in the Rock Physics Research laboratory, Twin Cities Mining Research Center. Friction characteristics of mineral (Al_2O_3) on rock under laboratory controlled conditions were used to provide basic knowledge for future improvements in efficiency of drilling and fragmenting of lunar materials. A large volume of information has been published (1-2)⁴

⁴Underlined numbers in parentheses refer to items in the list of references at the end of this report.

on the frictional behavior between metal/metal pairs. Research on the

rock/rock friction, however, has received very little attention. It was not until the early sixties that researchers started investigating the frictional characteristics of rock/rock interfaces (3-5). Since then, several studies (6-12) of friction between rock/rock interfaces under various conditions have been made but none of them evaluate the effects of the lunar environment.

This paper presents the experimental results of surface friction between a mineral probe and nine types of rock and two stainless steel specimens. Friction was measured in atmospheric, ultrahigh vacuum, and dry nitrogen environments. For each environmental condition two temperature levels (ambient and lunar day (135° C)) were considered. For each mineral probe/specimen pair, the friction was measured for both new track (NT) and same track (ST) tests. In the NT test, the mineral probe traveled along a new track for each test in the set whereas the probe in the ST test traveled along the same track on the specimen surface for every test in the set. The NT test simulated the friction between a moving object and the virgin surface. Any original surface condition which might affect the friction coefficient (that is, water molecules, surface oxide film) were present at each test. The objectives of the ST test were twofold: (1) the frictional effects on the rock surface caused by gradually removing any contaminating layer (for example, water vapor, oxide) and (2) the possible effect of cumulative debris generated during each test run on the frictional characteristics.

Since the exact surface state of rock on the Moon was little known at the time this work commenced, the worst possible testing criteria were considered to be those conditions which would present an ultraclean surface indicating a totally outgassed material. Such an ultraclean surface condition for the test samples was considered, for purposes of this project, to be the "worst case" testing condition. This testing was performed on the assumption that the Moon's exposure to hard vacuum, radiation, and particle bombardment over a long geologic time span had produced a lunar surface that was totally outgassed to a considerable depth thereby producing rock surfaces that approached an atomically clean condition. The intent of the research being presented was to approximate this hypothesized condition as closely as possible for maximum validity of test results.

Experimental Apparatus and Procedures

Equipment used for this research included an ultrahigh vacuum (UHV) system for lunar vacuum simulation to 5×10^{-11} torr and auxiliary measurement devices for accurately determining conditions in the UHV chamber during testing, a specially designed experimental apparatus for measuring friction between mineral/mineral or metal/mineral pair and associated data acquisition system (fig. 1). In addition, a profilometer was used

FIGURE 1. - Environmental Control System for UHV Friction Studies.

to measure the surface roughness and waviness of the specimen before and after the tests.

The detailed design of the UHV system and friction measuring device has been published (16). Eleven specimens were mounted on the periphery

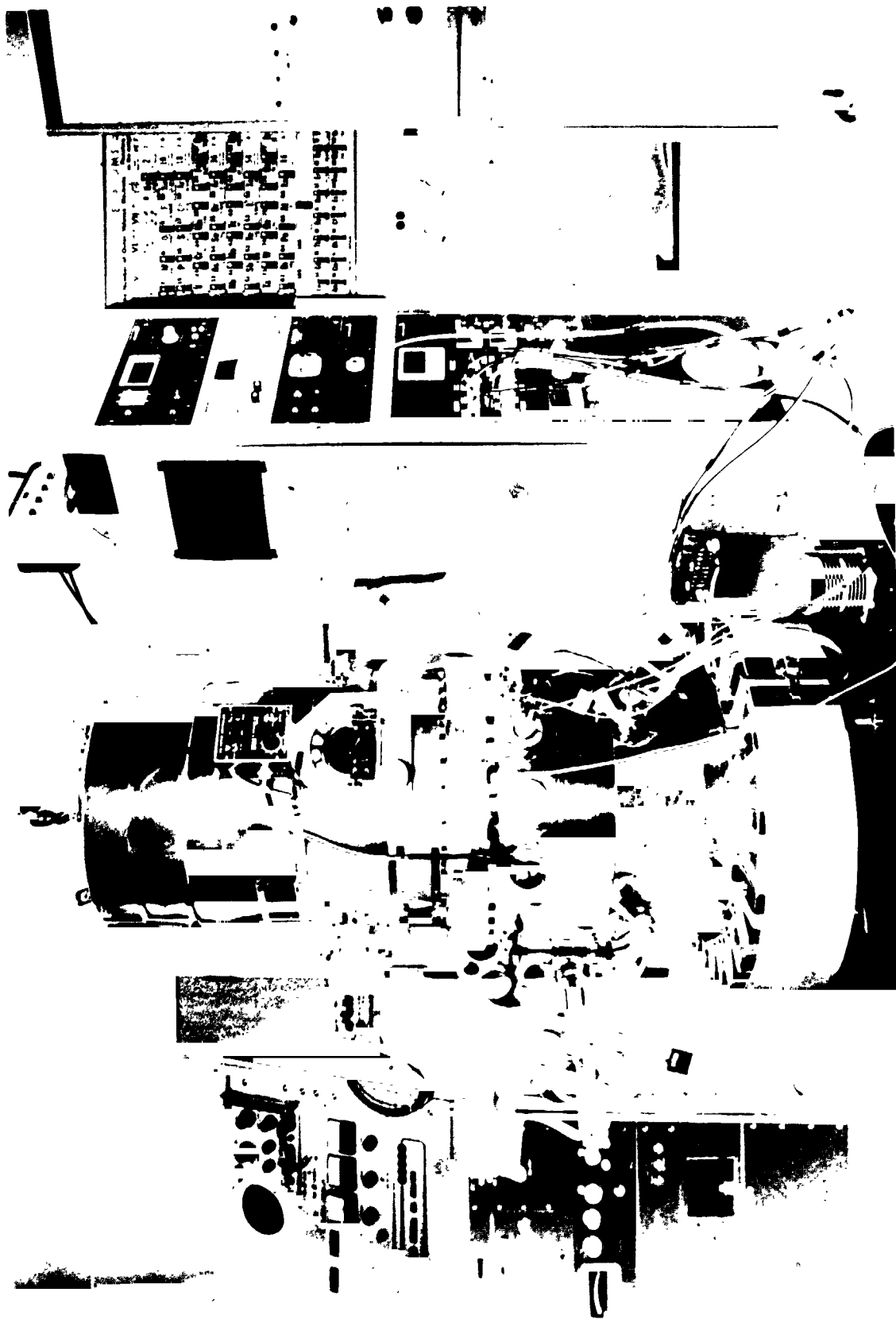


FIGURE I.- Environmental Control System for UHV Friction Studies

REPRODUCIBILITY OF THE ORIGINAL PAGE IS POOR

of a circular disk (fig. 2), which was rotated at a constant speed during

FIGURE 2. - Closeup View of Experimental Friction Apparatus.

testing. The friction measuring device was designed so that the position of the friction probe could be adjusted both horizontally to apply the normal load and vertically to vary the track position on the sample. This arrangement allowed several hundred tests on either the same or unused surfaces during one pump-down. The normal and tangential forces at the probe tip were recorded continuously during the testing.

The sapphire probe used was hemispherical with a radius of 0.032 inch. During testing, the position of the probe was fixed with a constant normal force of 100 grams applied against the test samples. The test samples were moved at a constant speed of 1.847 mm/min during each test. The normal force was chosen to maximize surface friction while minimizing effects caused by ploughing (1-2). This nominal force was proved valid as shown in the TV monitoring to be discussed later. Since friction is dependent on temperature induced at the interface, high speed of specimen rotation was not desirable, thus a nominal low speed was chosen. Only one normal load at one nominal speed was used to limit the test volume. In each test the tangential frictional force and the normal force (100 grams) were continuously monitored on separate analog channels as the probe traveled on the specimen surface for a distance of approximately 14 mm. The tangential forces will vary from point to point over the specimen surfaces tested, whereas the normal force remains constant. Continuous output of the ratio of the tangential force to normal force was plotted as a curve

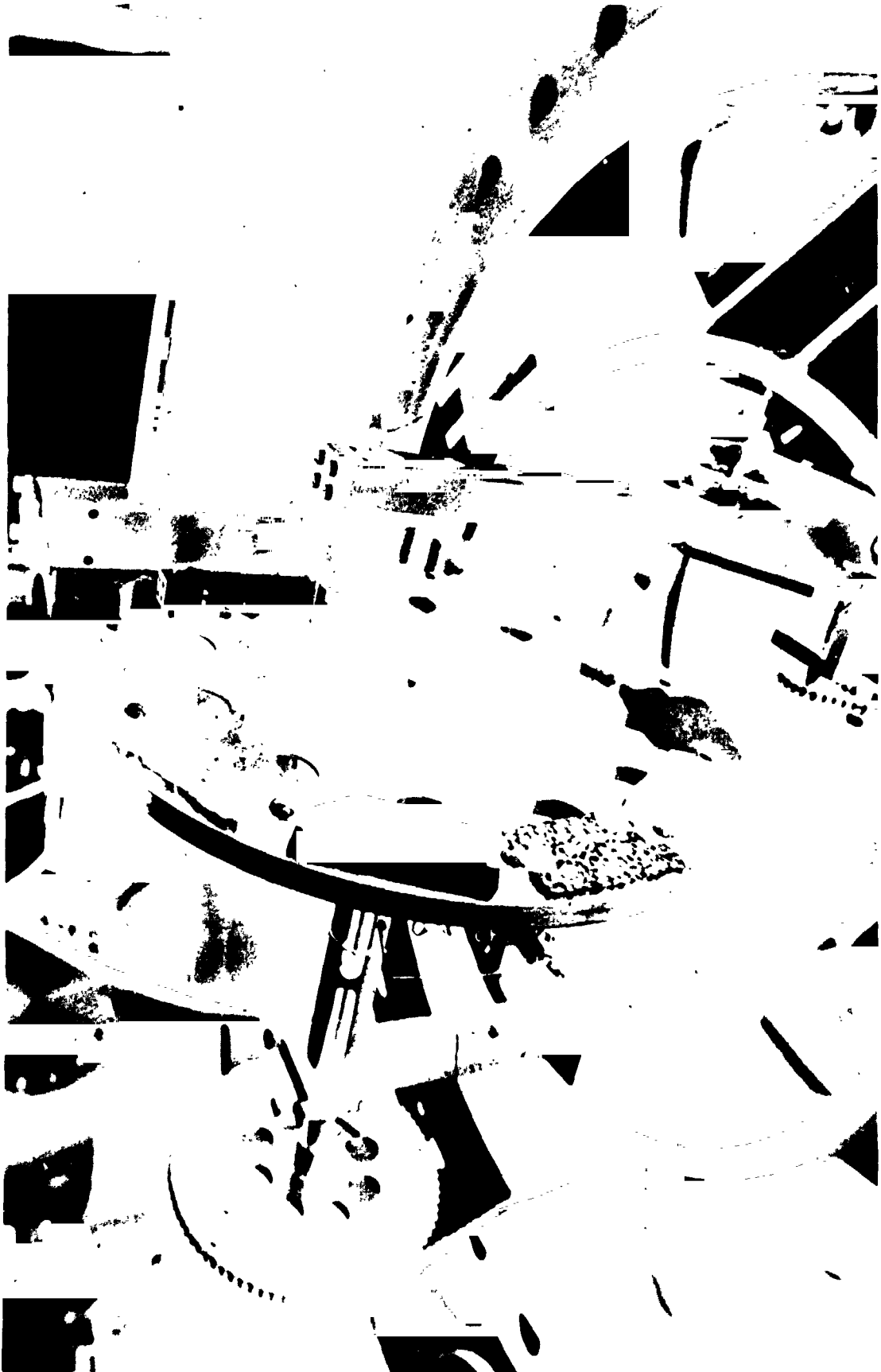


FIGURE 2.- Closeup View of Experimental Friction Apparatus

REPRODUCIBILITY OF THE
ORIGINAL PAGE IS POOR

on a strip chart recorder. The area under this curve was integrated electronically and plotted as another curve to obtain the total area. This total area was then divided by the total chart distance covered in the test to give the average area under the curve. This average area was then converted to the average kinetic coefficient of friction, μ_k , through calibration.

Each friction measurement was performed under several different conditions. Three environments--atmospheric, dry nitrogen, and UHV--were each used with two different temperatures--ambient and 135° C. All these environments were produced and tests were conducted in the same UHV chamber. The chamber provided an ideal test vehicle even at atmospheric condition because it prevented fluctuations which might otherwise be caused at the strain gage bridges by convective air currents. A supplementary air conditioner and a dehumidifier were used to help control the ambient environmental conditions. Temperature was maintained at 22° \pm 1° C in the laboratory. The UHV system was never opened when the relative humidity exceeded 35 pct (6.8 g/cu m of water vapor, absolute), at 22° C.

All μ_f tests performed at ambient or elevated temperature in UHV and atmospheric conditions consisted of sets containing 10 to 20 measurements for each sample. Since quartz was used as a standard reference the largest data sets were obtained for this material. The sets for atmospheric pressure at elevated temperature and dry nitrogen ambient and elevated temperature conditions consist of one, two, and three measurements, respectively,

because they prove to be within the trend indicated by earlier tests in the other environmental conditions. In ST testing, friction results were only obtained under dry nitrogen and UHV conditions. Only one set of data was obtained for each sample, that is, tests were performed on one trial and consequently the friction data shown later were not the average values of several measurements as those in NT tests. A set of data consists of 3 measurements for dry nitrogen at elevated temperature and 6 measurements for dry nitrogen at ambient condition, whereas 10 to 16 measurements were made under both UHV ambient and elevated temperature conditions.

Specimens and Specimen Preparation

Based on the results obtained by others (13-14) from lunar photometry, radar, and telescopic observation, the U.S. Bureau of Mines, Twin Cities Mining Research Center established a standard suite of igneous rocks (15-16) which most closely simulate the lunar materials. Among these rock types, the tholeiitic basalt was closest to the chemical analysis of the returned lunar materials (16). Accordingly, tholeiitic basalt was chosen as the major test material. The other materials chosen for this study were major minerals within basalt or they provided reference points which could be verified in the literature. Andesine, feldspar, labradorite, magnetite, and pyroxene fall into the first category whereas quartz and stainless steel fall into the second one. Two types of stainless steel specimens were used: one with surface polished

with $0.03 \mu\text{m Al}_2\text{O}_3$, and the other with $40 \mu\text{m Al}_2\text{O}_3$. Dacite was chosen for this study also, because of its outgassing characteristics, even though it does not fall into either of the two categories mentioned. Outgassing effects were considered essential to stabilize samples at equilibrium with the vacuum environment. Therefore, a considerable effort was made prior to beginning the friction testing to establish these outgassing characteristics. This work, reported earlier (17-18), showed that dacite outgasses very easily due to its high porosity while basalt outgasses more slowly since it is much denser. This means that dacite cleans up interstitially in the UHV quite easily while the basalt keeps recontaminating the surface by interstitially contained water vapor migrating to the surface. This effect is readily seen in some of the data presented later.

To most nearly approach the pristine lunar condition during UHV testing, specimen preparation was very carefully controlled. All sizing and finishing was done using only water as the lubricant. While this is not a desirable element in the finished specimen it is easier to handle than vegetable base oils which are not as easily baked out. The samples were cut in thin slabs ($1/8$ inch thick by $1-1/2$ inches long by $3/4$ inch wide) from the bulk material. The surfaces were lapped by stages to a final finish with 400 mesh Al_2O_3 ($40 \mu\text{m}$). All surfaces, except one stainless steel reference specimen, received the same surface finish. The steel reference specimen had a surface polished with $0.03 \mu\text{m Al}_2\text{O}_3$. The

relative surface textures for all of the test samples are shown in figure 3.

FIGURE 3. - Enlarged (X 10) View of the Specimens Showing Relative Surface textures: A. Sample Wheel With All Specimens Mounted in Position (X 1/3), B. Andesine, C. Basalt, D. Dacite, E. Pink Feldspar, F. White Feldspar, G. Magnetite, H. Labradorite, I. Pyroxene, J. Quartz, K. Stainless Steel, and L. Stainless Steel (Polished).

Figure 3A shows the sample wheel with all samples mounted for direct comparison. The remaining figures are enlargements (X 10) of the surfaces to show the individual textures. After polishing, these specimens were placed in a low vacuum oven (10^{-3} torr region) and baked at 135° C for several weeks. Since the maximum temperature on the lunar surface has been found to be 135° C, the specimen conditioning and any bakeout in the UHV system did not exceed this temperature. After this extensive bakeout for initial degassing, the vacuum oven was backfilled with a prepurified (ultra dry) dry nitrogen. The dry gas filled all voids, pores, and interstices in the specimens during cooling and helped prevent more than surface water vapor contamination during final transfer from the oven to the UHV system.

EXPERIMENTAL RESULTS (ST, NT)

Figures 4 and 5 show the typical traces of kinetic coefficients of

FIGURE 4. - Typical Dynamic Friction Traces for Atmospheric Room Temperature Condition.

FIGURE 5. - Typical Dynamic Friction Traces for UHV Room Temperature Condition.

friction of dacite, quartz, and stainless steel at atmospheric and UHV

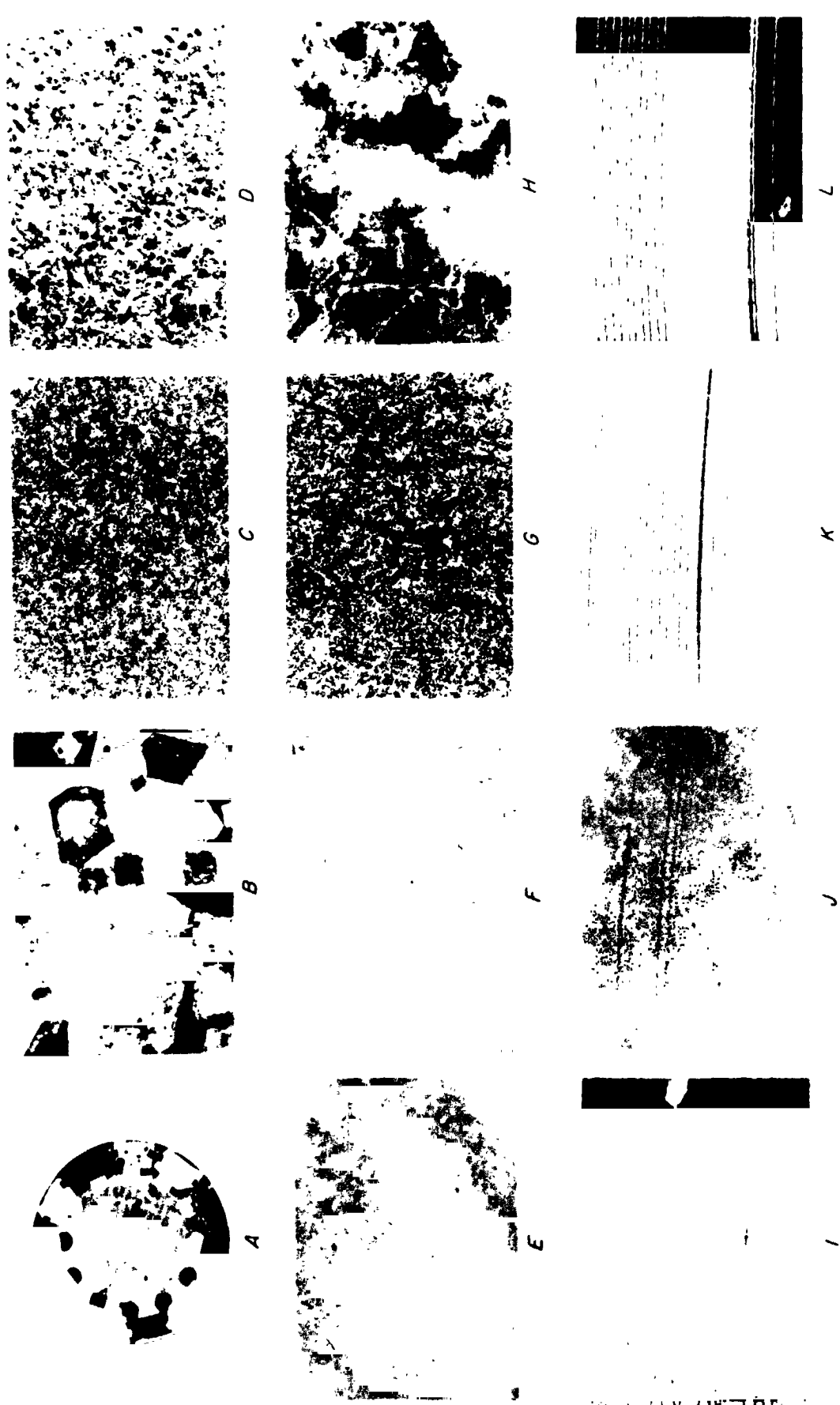


FIGURE 3.- Enlarged (X 10) View of the Specimens Showing Relative Surface Textures

REPRODUCIBILITY OF THE ORIGINAL PAGE IS POOR

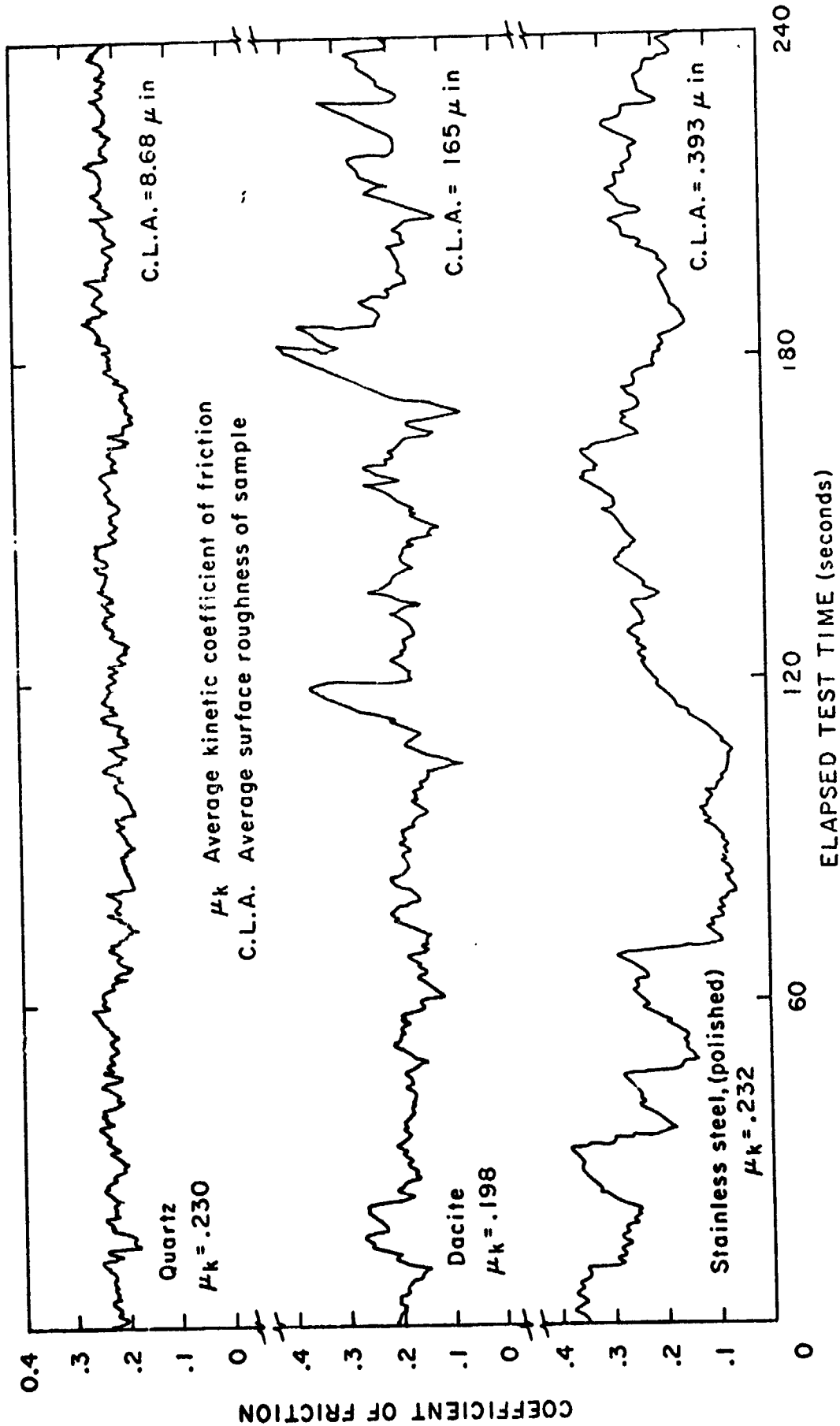


FIGURE 4. - Typical Dynamic Friction Traces for Atmospheric Room Temperature Condition.

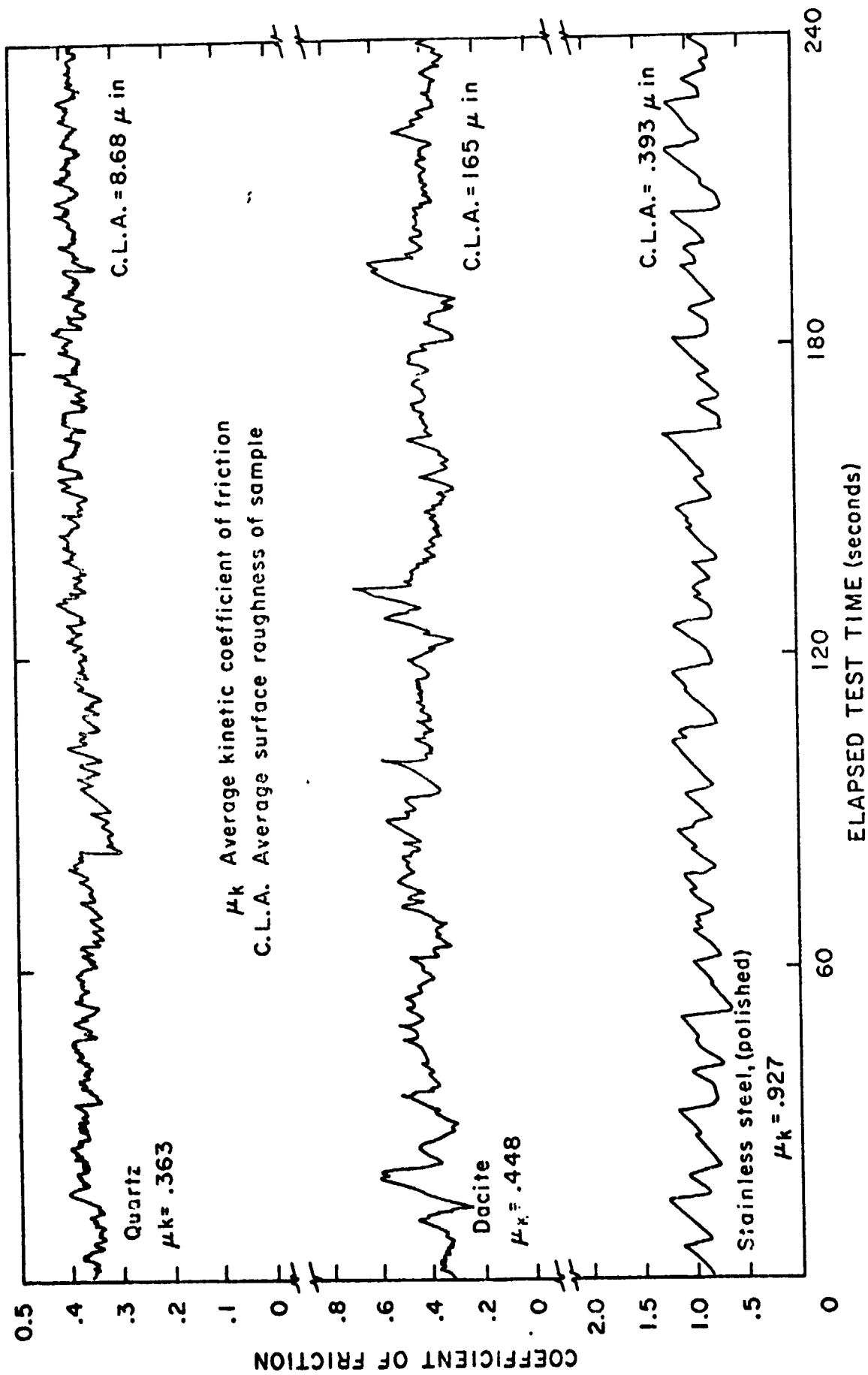


FIGURE 5. - Typical Dynamic Friction Traces for UHV Room Temperature Condition.

room environments, respectively. The instantaneous coefficient of friction varied from point to point on the specimen surface with the variations often being very large. This was especially true for dacite and stainless steel specimens. The variations for quartz were much smaller. The areas under these curves were electronically integrated over the testing distance (1.5 cm) from which the median value was calculated to provide the kinetic coefficient of friction. Figure 6 shows the average

FIGURE 6. - Average Friction Values for New Track Test in Three Environments.

values of friction (μ_k) for all samples as a function of the environmental conditions for the NT tests. The black dots show the mean of that data set and the vertical bars represent the range of data obtained. A set of data may include 3 to 30 measurements depending on rock types and reproducibility (see appendix A). The deviation from the mean was the least under ambient atmospheric environment and greatest under UHV ambient temperature environment. Friction was lowest for all rock types under atmospheric ambient environment increasing slightly when heated to 135° C. Friction reached maximum with specimens under UHV room environment and dropped slightly when they were heated to 135° C under UHV condition with the exception of stainless steel and pyroxene. When the UHV condition was changed by backfilling the chamber with dry nitrogen, the friction values were between the two extremes of atmospheres and UHV conditions for all rock types tested except for pyroxene and stainless steel. Under the nitrogen condition, as the temperature was increased friction increased or decreased depending on rock type.

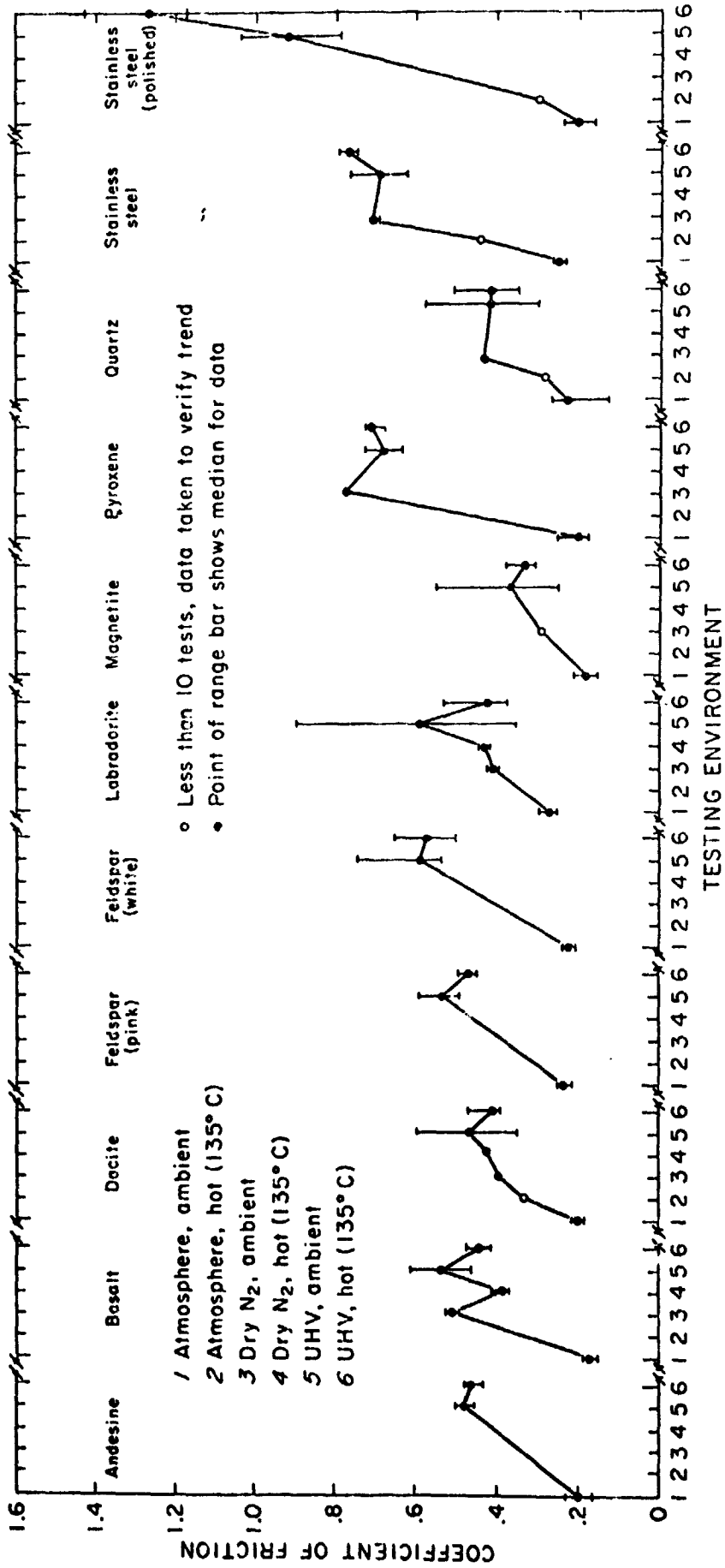


FIGURE 6. - Average Friction Values for New Track Test in Three Environments.

Figures 7 to 12 show the results of ST tests. For mineral and rock

FIGURE 7. - Friction Measured Under Same Track Tests for Basalt and

Magnetite,

FIGURE 8. - Friction Measured Under Same Track Tests for Dacite and

Labradorite.

FIGURE 9. - Friction Measured Under Same Track Tests for Feldspar.

FIGURE 10. - Friction Measured Under Same Track Tests for Stainless Steel.

FIGURE 11. - Friction Measured Under Same Track Tests for Quartz and

Pyroxene.

FIGURE 12. - Friction Measured Under Same Track Tests for Andesine.

specimens, the friction increased during the first several runs and then tended to level off regardless of the environmental conditions under which tests were conducted. The stainless steel did not show this pattern but indicated a continuous decrease instead. The rate of increase during the initial runs on mineral and rock specimens and the numbers of the run where friction begins leveling off differed with each sample type. Generally speaking, the shapes of the curves for a particular sample show a common trend under different testing environments.

DISCUSSION

Friction measured at atmospheric ambient environment during NT tests was generally the lowest for all sample types in any environment and had the smallest scatter in each set of data. This was due to the existence of water vapor and other contaminating films, that is, oxide, which act as lubricants on the specimen surfaces (1-2). With the exception of stainless steel and pyroxene, friction was highest for all sample types when

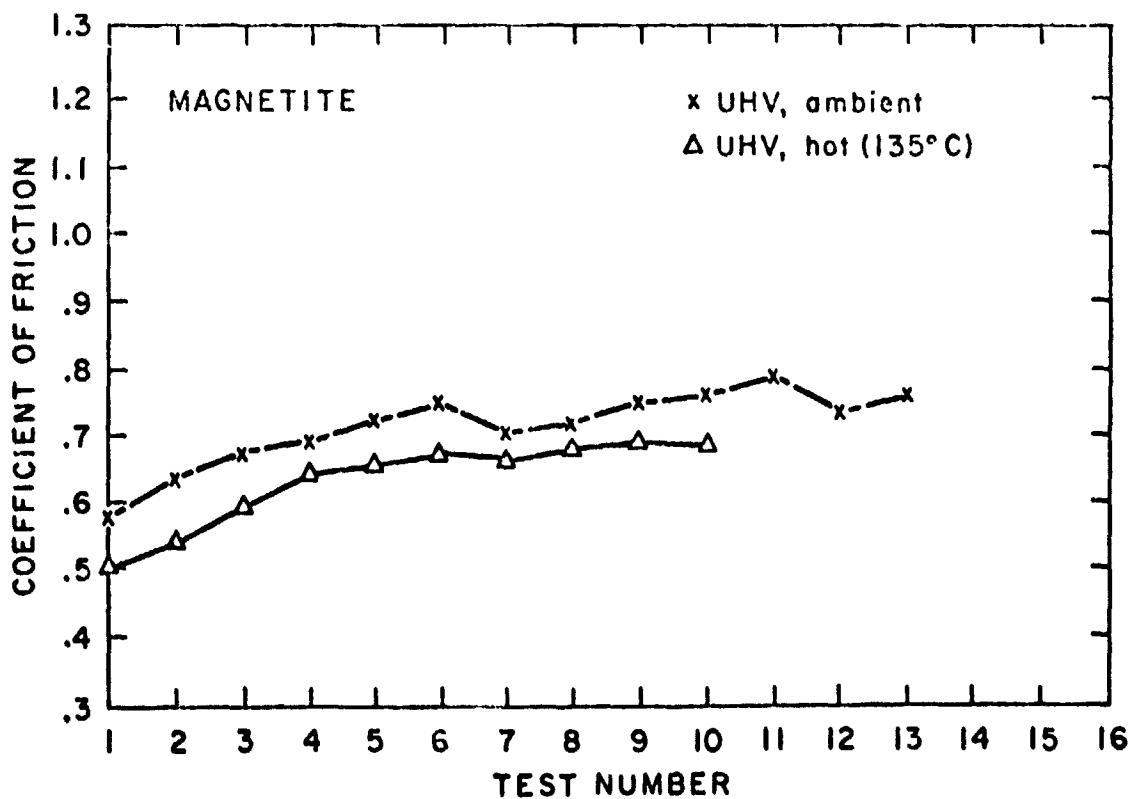
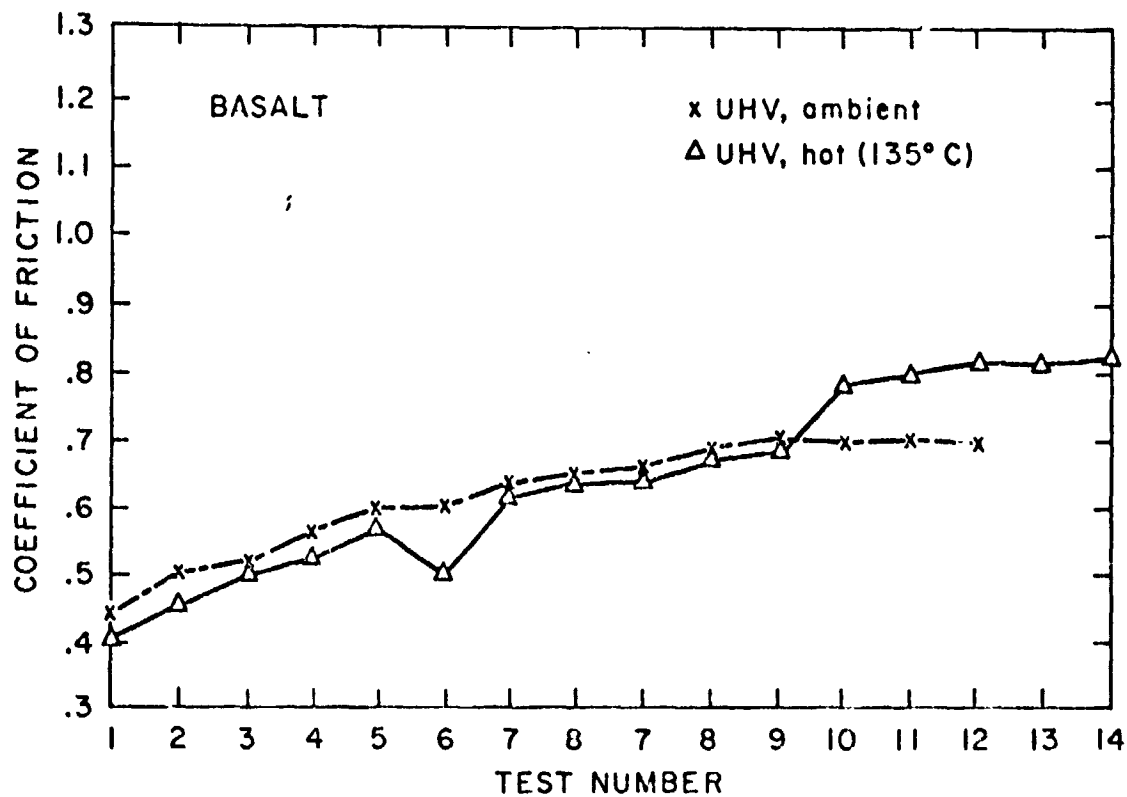


FIGURE 7. - Friction Measured Under Same Track Tests for Basalt and Magnetite.

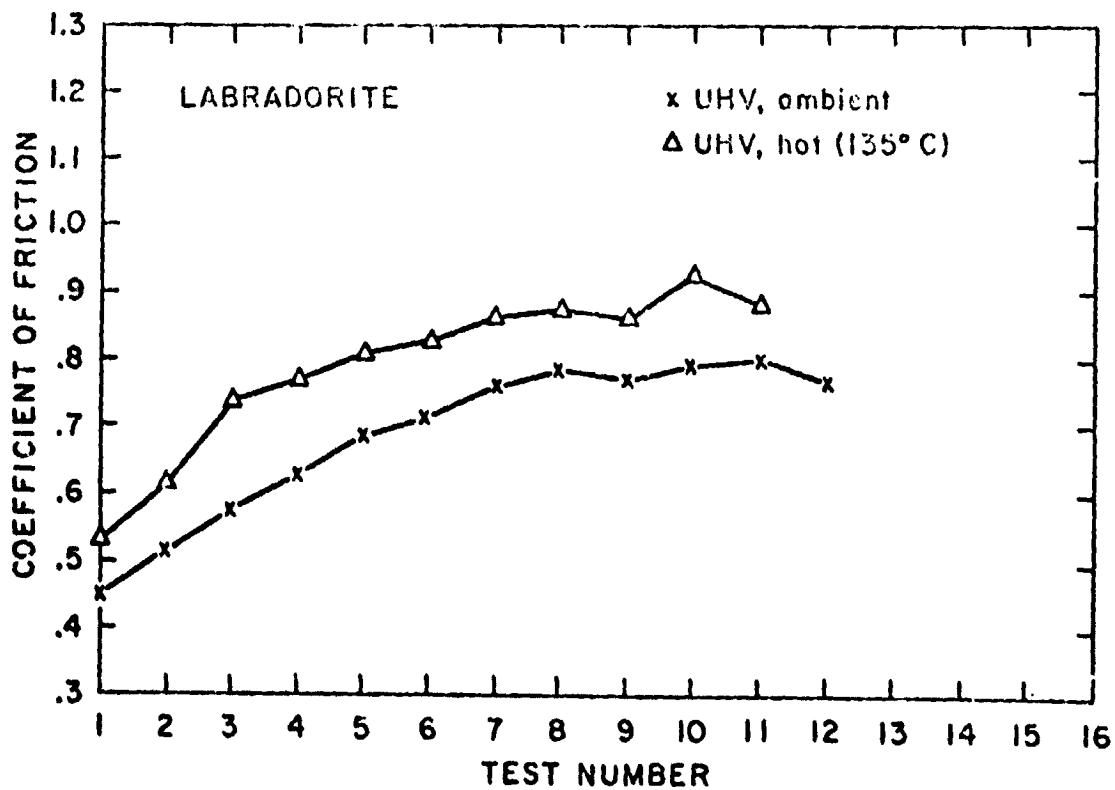
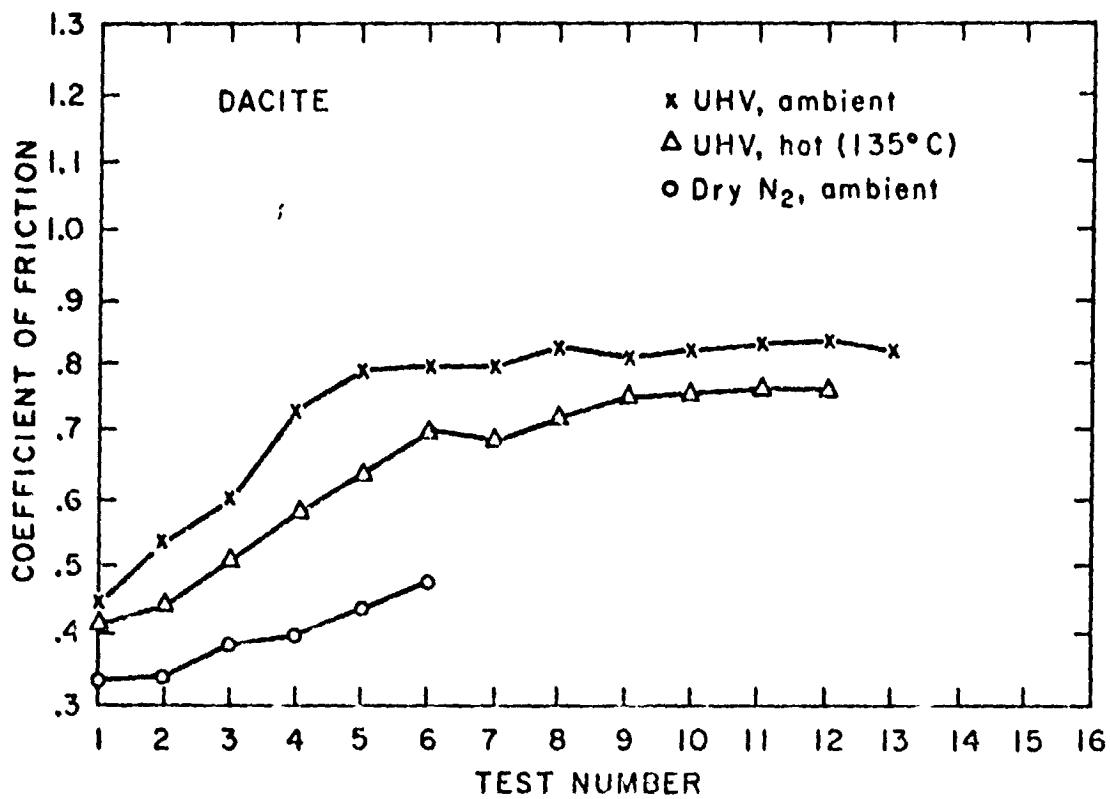


FIGURE 8. - Friction Measured Under Same Track Tests for Dacite and Labradorite.

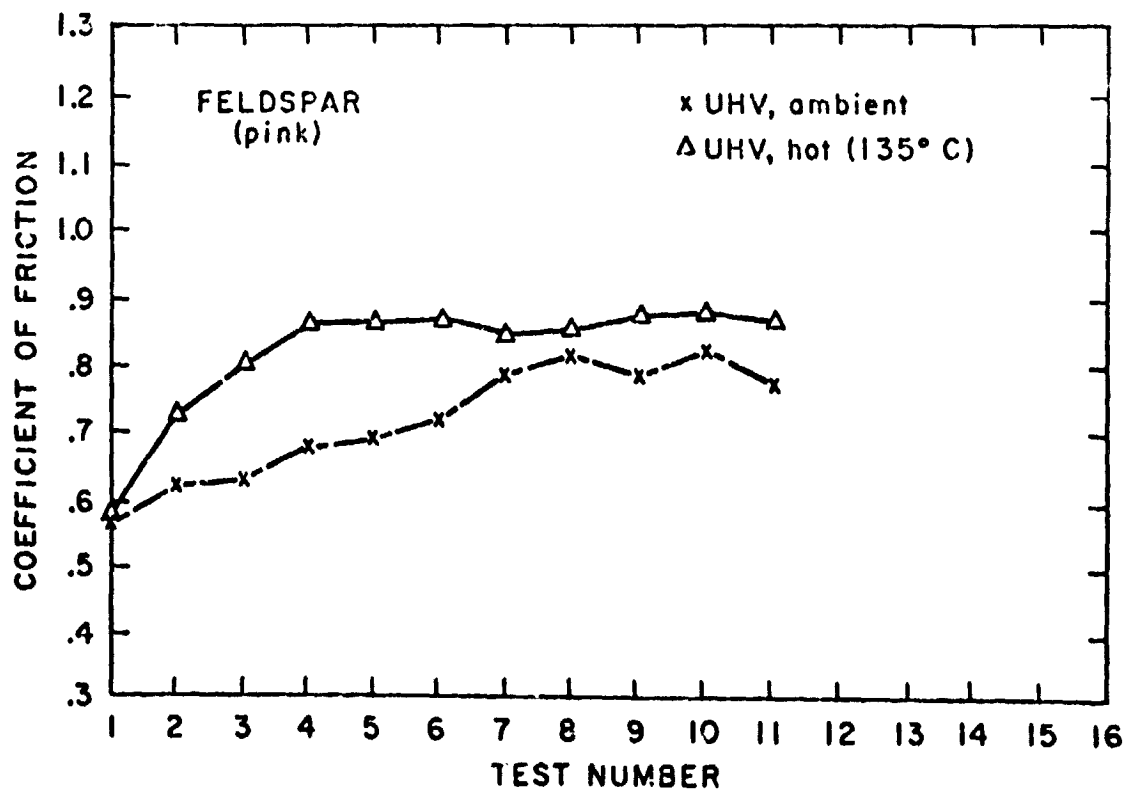
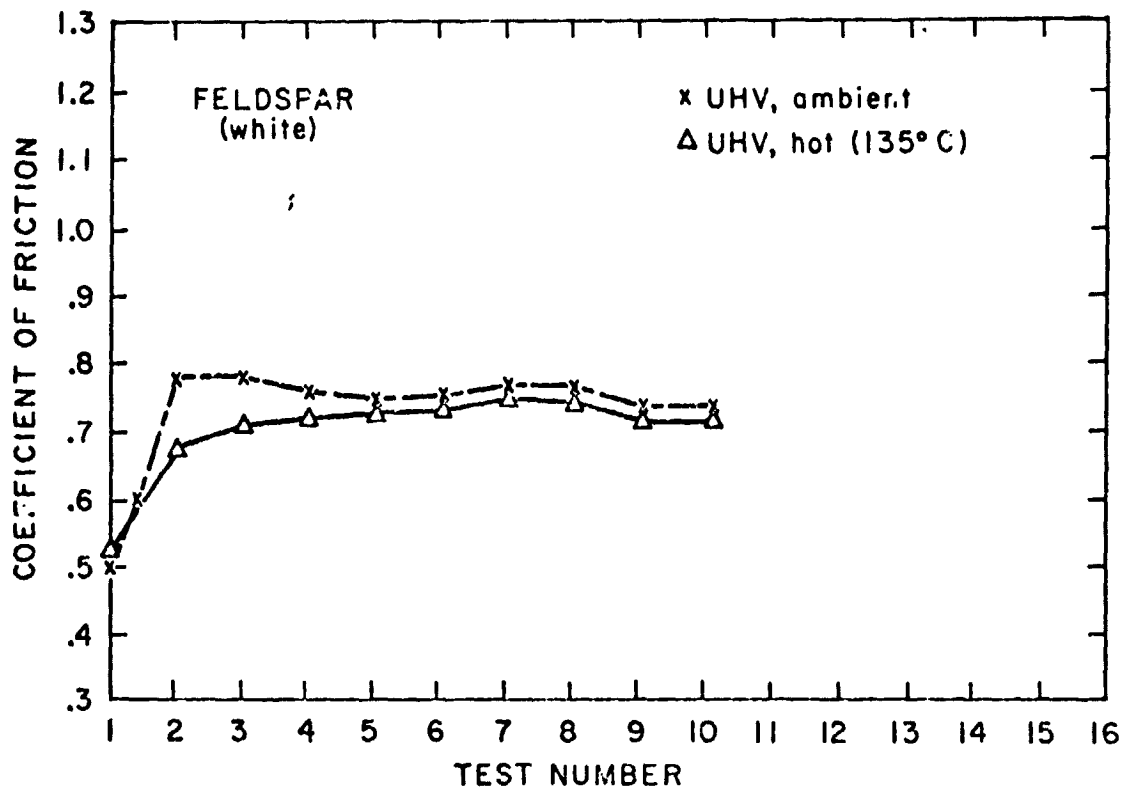


FIGURE 9. - Friction Measured Under Same Track Tests for Feldspar.

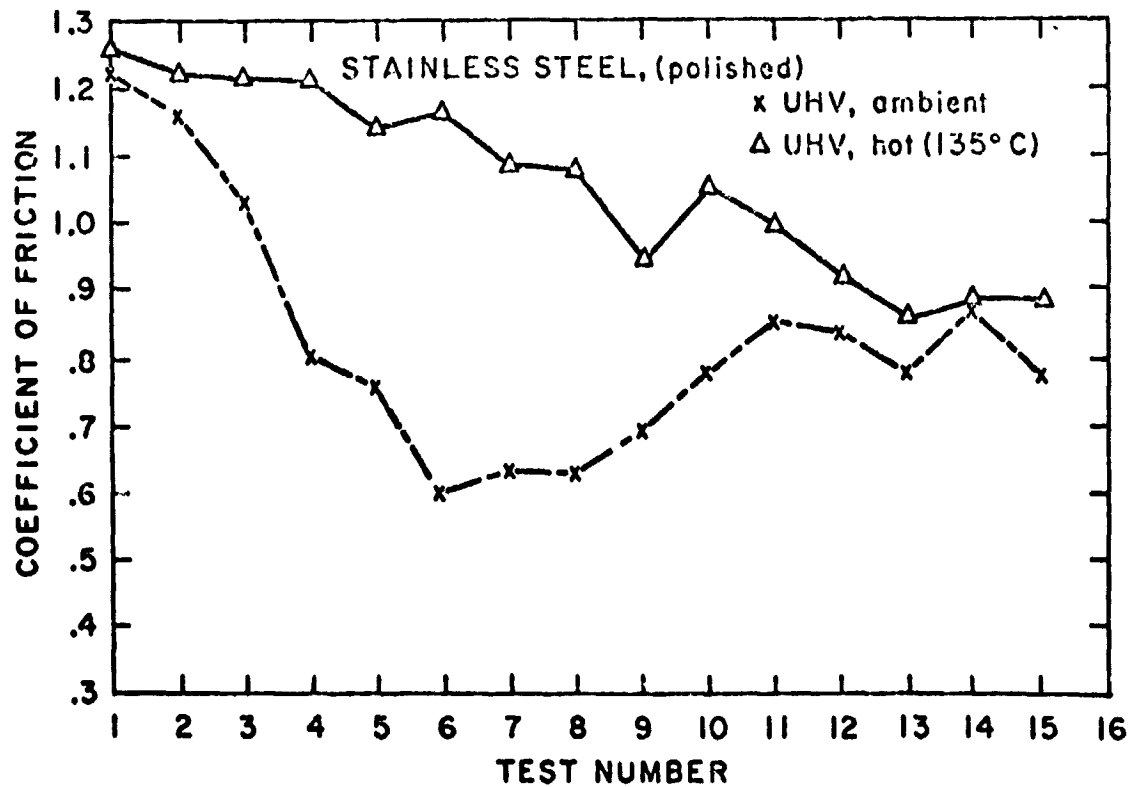
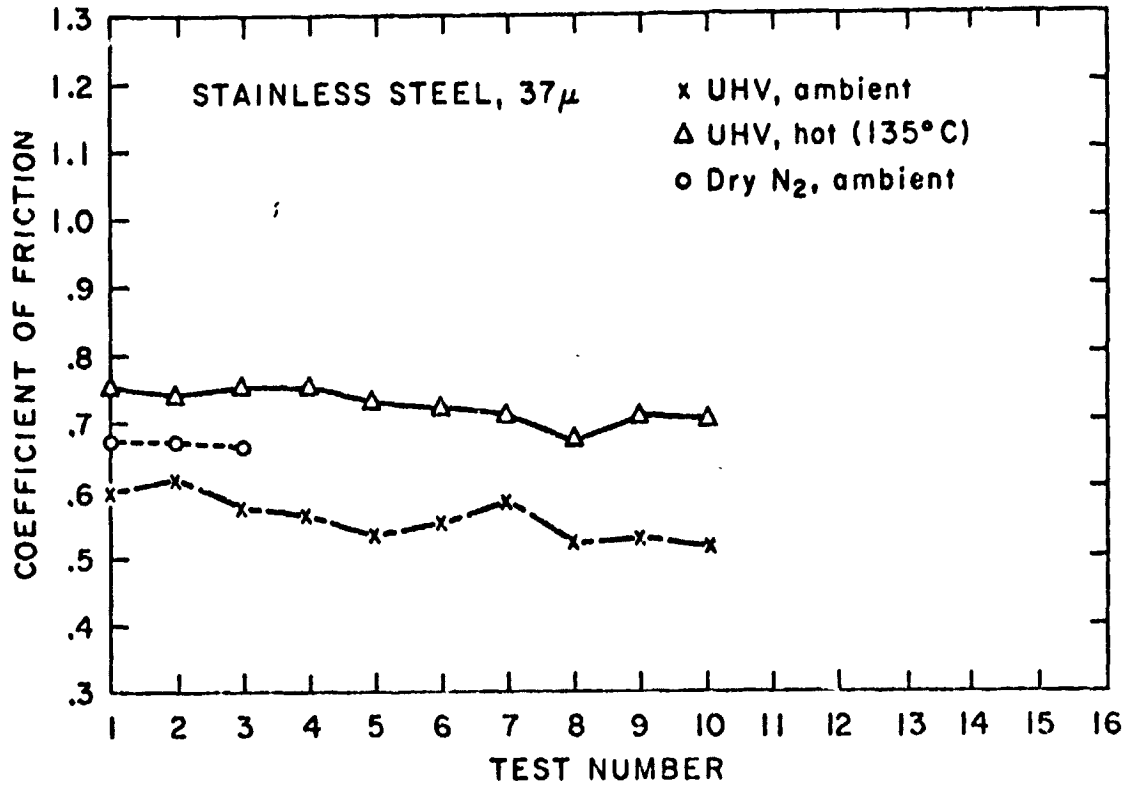


FIGURE 10. - Friction Measured Under Same Track Tests for Stainless Steel.

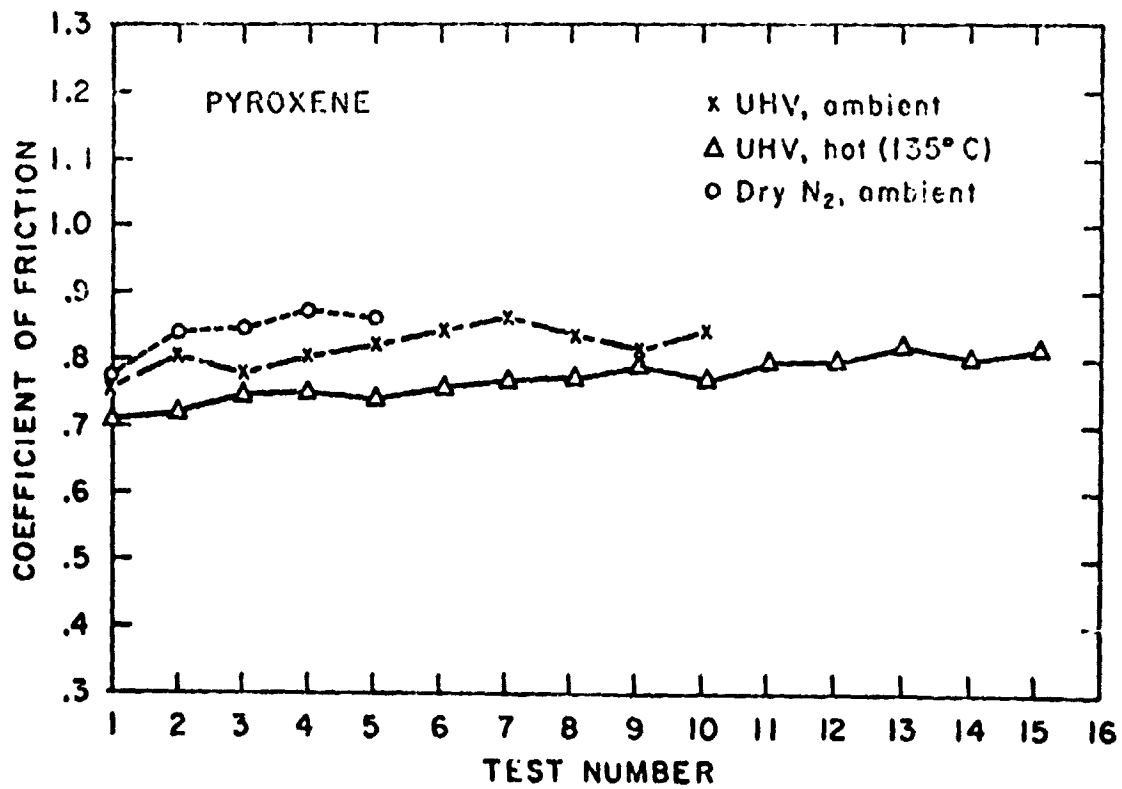
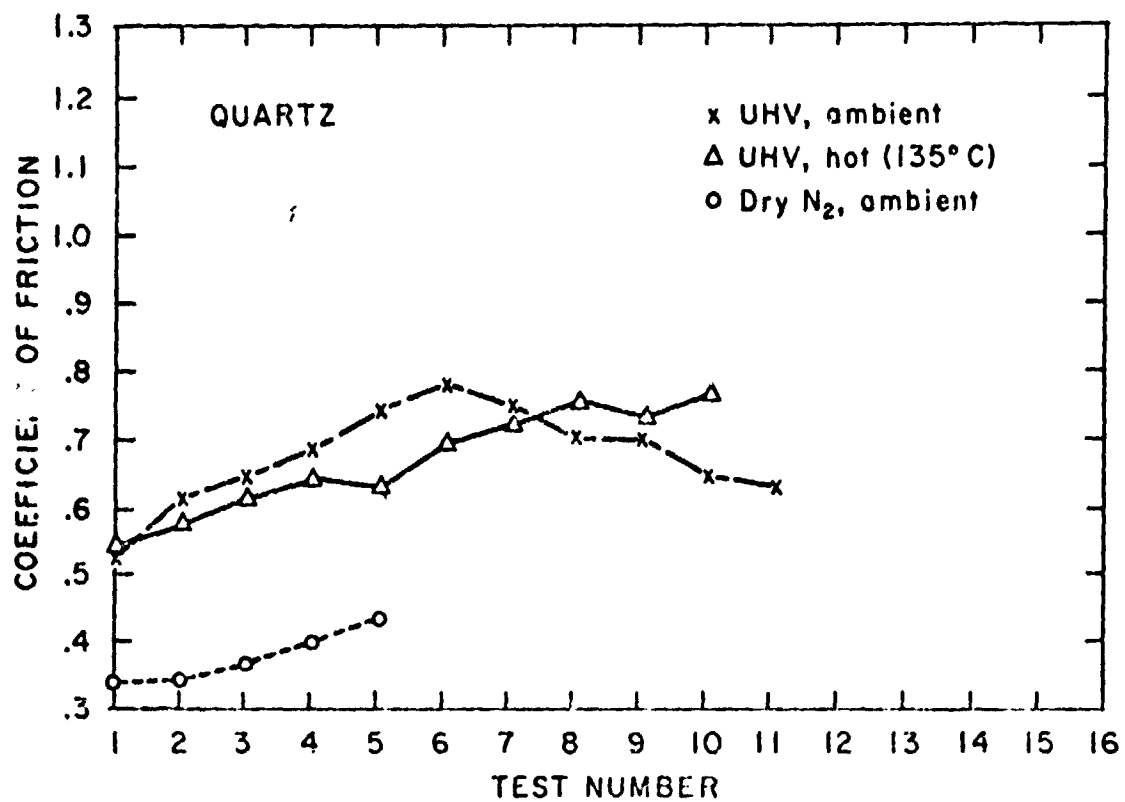


FIGURE 11. - Friction Measured Under Same Track Tests for Quartz and Pyroxene.

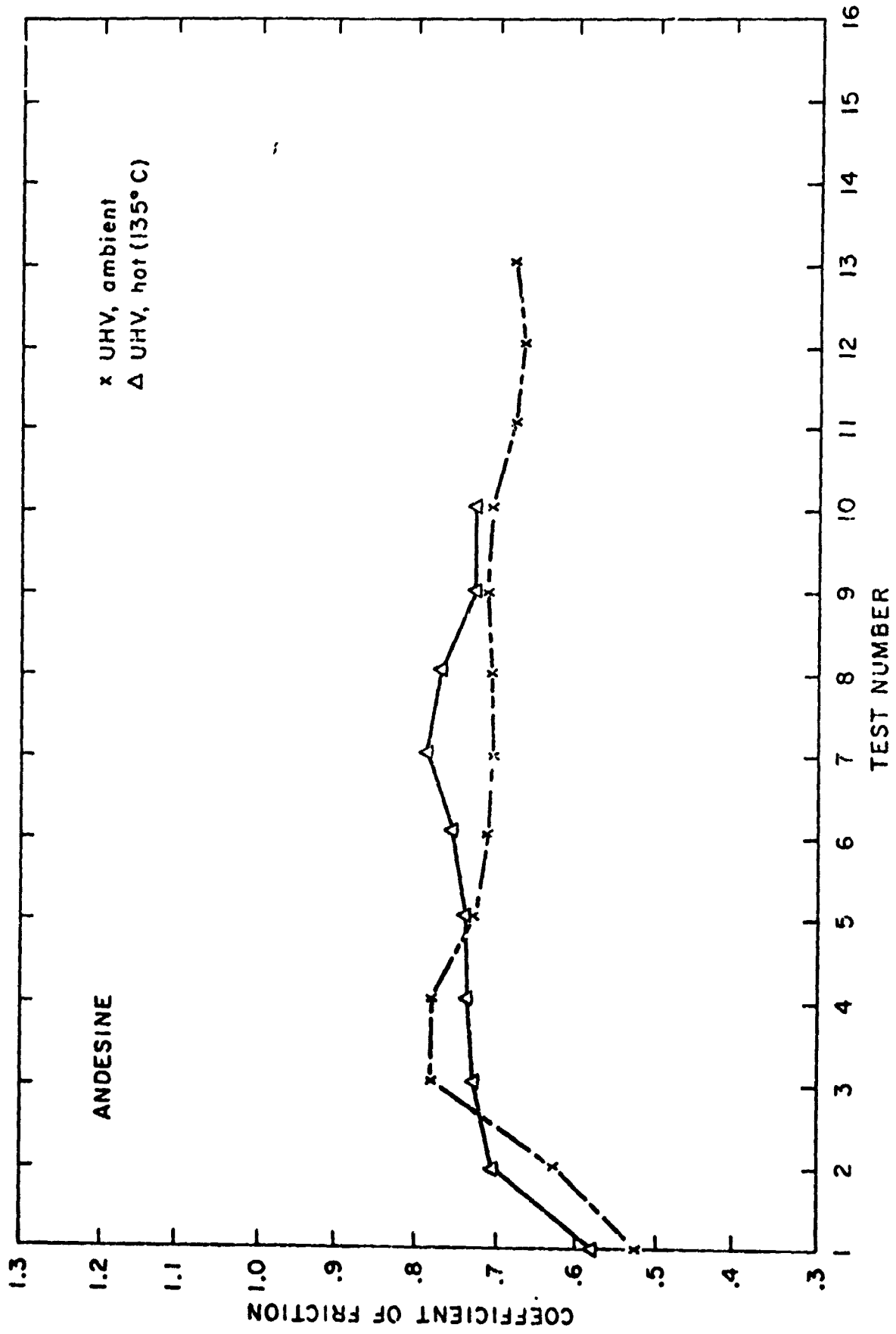


FIGURE 12. - Friction Measured Under Same Track Tests for Andesine.

tests were conducted in UHV ambient temperature condition. This increase in friction value varied for each sample type but ranged from twice that obtained in atmospheric ambient temperature condition for quartz to 3.6 times for polished stainless steel. These increases in friction were presumably due to the highly cleaned surfaces produced in UHV by removal of surface water vapor and other contaminants (19), thus more intimate contact at the mineral/rock or mineral/metal interface was achieved. When the UHV testing chamber was backfilled with dry nitrogen at ambient temperature, the frictional values remained approximately the same as those obtained in UHV ambient temperature condition for quartz and stainless steel, but increased for pyroxene and decreased for basalt, dacite, labradorite, and magnetite. These mixed effects for different rock types may be partially caused by some inevitable water vapor contaminant in dry nitrogen although the manufacturer claims that the dew point of the pre-pure dry nitrogen is better than -90° F. When specimens in these three environments are heated to lunar day temperature (135° C), several physical and chemical effects could occur in the specimens to change the frictional values. These effects include the reduction in strength of the asperities, interstitial water vapor driven to the specimen surfaces, and a change in character of the existing contaminating films, thereby causing changes to occur in the adhesive strength of the contact junctions at the interface (1). In the atmospheric elevated temperature condition, the friction was larger than that in atmospheric ambient temperature condition for dacite, quartz, and stainless steel. The same increases in friction were seen for dry nitrogen ambient to the dry nitrogen elevated temperature condition except for basalt where considerable decrease occurred.

The increase in temperature in these two conditions (atmospheric and dry nitrogen) removed more water vapor from the specimen surface than arrived from the interstitial water vapor. Additionally, although the asperity strength was weakened appreciably (20), it is hypothesized that the net effect was an increase in adhesion strength of the junction contacts due to characteristic changes of the contaminating films. In basalt, the dominating factor seemed to be a summation of both effects. Since the low porosity of basalt provided slower outgassing, it is possible that sufficient contained water vapor remained interstitially to provide a lubricating film in addition to the decrease in asperities strength accounting for a marked decrease in friction. In UHV elevated temperature condition, the specimen surfaces were presumably at least as clean as those in UHV ambient temperature condition because the interstitial water driven to the surface tended to vaporize more readily. Therefore, the decrease in friction in UHV elevated temperature as compared with those in UHV ambient condition for most rock types was likely due to the decrease in asperities strength (20). No effect on asperities strength would be expected for stainless steels at this low temperature. The reason for the reverse effect on pyroxene is unknown at this time. The visible track marks shown only in these specimens (fig. 3I-3L) indicate that ploughing action could play a large role.

Under the ST tests, with the exception of stainless steel the friction value on the first test was always the lowest. It increased either gradually (for example, quartz) or sharply (for example, white feldspar)

depending on sample types during each subsequent run. The friction became stabilized at some higher value at a point between the second run, (white feldspar) and the seventh run, (labradorite). Stabilized friction values were: 1.98 times the first run for basalt, 1.8 for dacite, 1.39 for quartz, and 1.16 for pyroxene. A videotape made through a microscope at X 50 indicated that normally no visible debris was generated by the probe and specimen contact. This did not preclude the production of microscale dust particles, however, which might accumulate during each run and increase the friction and wear during succeeding tests. Another event occurring simultaneously during the time the probe travels along the same track was the damage to the contaminant film. The film was removed or depleted until the friction reached its highest point and stabilized. These two factors contributed to the highest stabilized values of friction which were obtained in this research.

The general trends of environmental effect on friction in rock/rock or rock/mineral interface as seen in NT tests were repeated in the ST tests for andesine, basalt, dacite, white feldspar, magnetite, pyroxene, and quartz. Reverse trends were seen for the other samples. This did not mean the conclusions for the NT test were invalid, because test data in UHV room temperature condition had the largest scatter (fig. 6) and the data in ST test represented only a single test run. As shown in figure 10 an opposite effect was seen for stainless steel. Friction on the first run was the highest and decreased linearly during the subsequent runs. The reduction in friction, however, did not seem to reach stabilization within the test runs.

Surface profiles of the specimens tested were mapped both before and after the tests. In figure 13 typical surface profiles for polished stain-

FIGURE 13. - Typical Surface Profiles Used to Obtain Average Surface
Roughness (C.L.A).

less steel, quartz, and dacite are shown. They were traced along sections perpendicular to the frictional tracks. No significant waviness was found for any specimen. No trace of friction tracks left behind by the probe was detected for any specimens except the stainless steels, pyroxene, and quartz. The other surface profiles, therefore, appeared essentially unchanged. The average surface roughness for each specimen is shown in table 1 together with Shore hardness measurement. Dacite was the roughest with 165 μ in while the polished stainless steel was the smoothest with 0.394 μ in. The apparent inverse relationship between Shore hardness and roughness indicated that the harder the specimen, the smoother the surface. Since all the specimen surfaces were prepared by using 40 μ m lapping compound, the discrepancy in final surface roughness can be attributed to materials inhomogeneity and porosity. The harder components erode less while the adjacent softer components (matrix) wear more, and the more porous the material, the rougher the average value of the final surface appears. No direct correlation between surface roughness and friction was found, but this was expected based on works of others (21).

The videotaped friction experiments mentioned previously were done to provide a more detailed study of the mechanisms of friction. A photograph

TABLE 1. - Average surface roughness and Shore hardness
(probe radius equals 0.0005 in)

	Shore hardness	Surface roughness	
		μ in	μ m
Stainless steel (polished)		0.433	0.011
		.354	.009
Quartz	122.15	8.680	.221
Stainless steel		9.570	.244
Feldspar (white)	107.30	11.850	.310
Labradorite	103.95	15.900	.405
Basalt	101.35	16.100	.410
Feldspar (pink)	109.65	17.150	.437
Pyroxene	72.30	17.900	.455
Andesine	103.10	26.100	.665
Magnetite	60.75	43.500	1.120
		39.300	1.000
Dacite	48.95	165.000	4.200

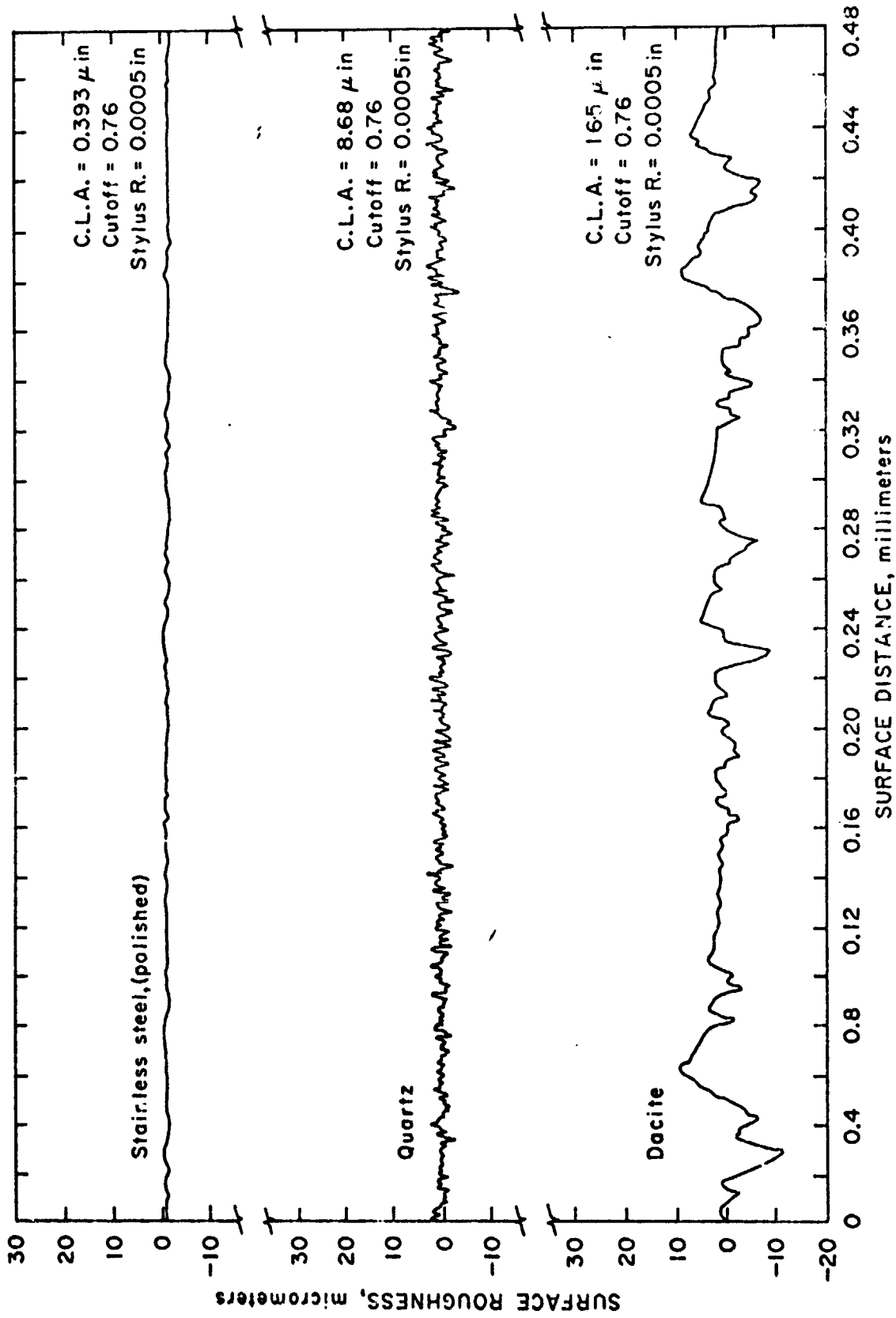


FIGURE 13. -- Typical Surface Profiles Used to Obtain Average Surface Roughness (C.L.A.)

taken of the TV playback (fig. 14) shows the friction probe sliding on

FIGURE 14. - Videotape TV Display of Friction Probe on Dacite.

dacite. The probe has a dark tip due to the light angle. No visible wear was found along the full track under normal conditions except, however, due to high porosity in the dacite. This porosity usually provides several pits along the track. When the probe drops into a pit, such as that seen to the upper right of the probe, it may produce chips at the leading edge and the normal load may be proportionally reduced if the pit is very large. The automatic data acquisition was so designed that the instant value of both normal and frictional force were used for obtaining the friction traces shown in figures 4 and 5 and any change in load would not cause a major variation in the average value of friction.

Current friction theories all state that the interface of two solids in contact consists of minute junction spots which carry the full load imposed at the interface. Therefore, the true contact area is always much less than the apparent geometric area. The existence of contaminant films between contacting junctions at the interface will cause further alteration in the true area of probe/specimen contact. Friction is the average value of the forces required to shear these junctions which are continuously being formed and broken during the course of sliding. Two basic phenomena may be associated with this average value of friction. One is that sliding on these junctions must be a discrete, discontinuous process. The numerous peaks and valleys on friction traces shown in figures 4 and 5 substantiate this. The other phenomenon is that the cleaner the surface, the more intimate contact becomes between the junctions which provides an increase in

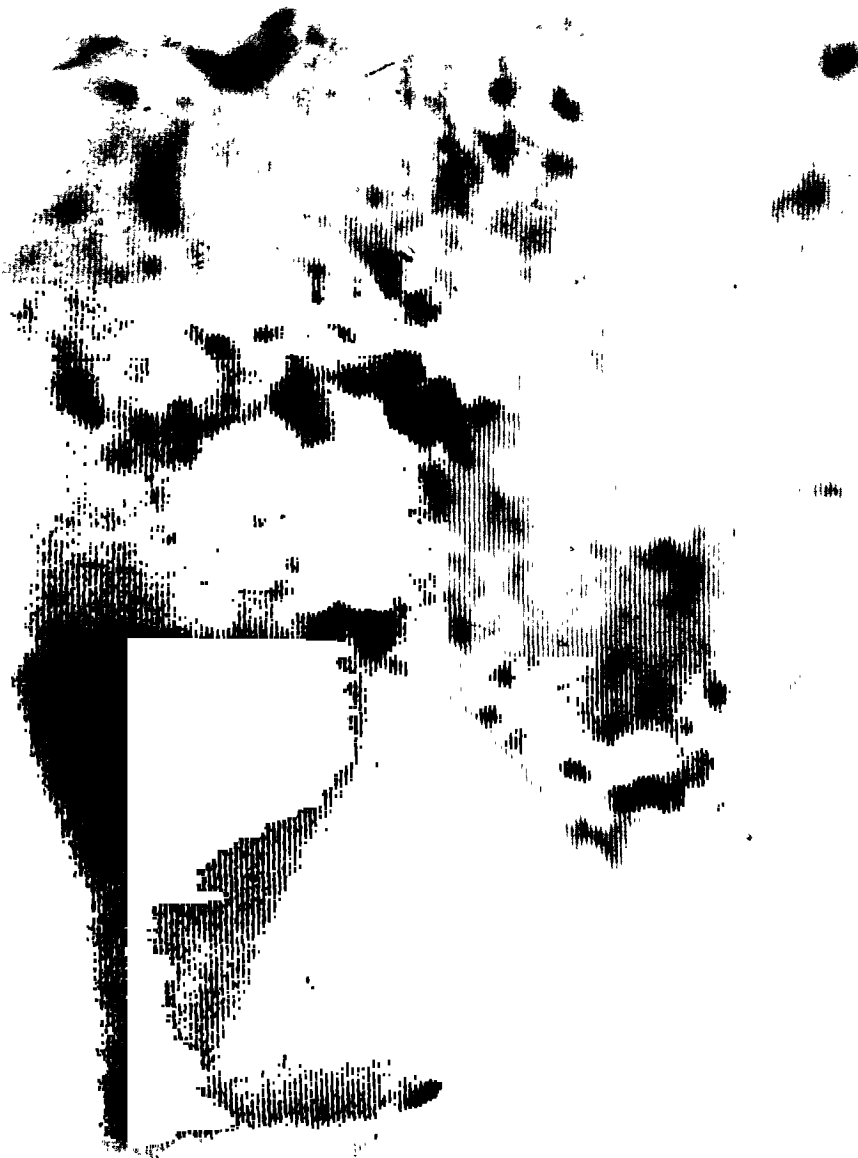


FIGURE 14.- Videotape TV Display of Friction Probe on Dacite

REPRODUCIBILITY OF THE
ORIGINAL PAGE IS POOR

friction. This was also observed in the study. Under UHV condition the surface is superclean resulting in more intimate junction contact. As a result, the friction under UHV is much higher than that under atmospheric condition. One specific point which deserves mention is that study followed the tradition in friction research by presenting the results in terms of a single-values friction coefficient. Since the coefficient of friction varied over a wide band (figs. 4-5), this single-valued friction number did not contain any information about the number of occurrences or magnitude of any given peak or valley in the friction traces. Therefore, two materials with the same average coefficient of friction (μ_k) can have two very different friction traces (figs. 4-5) and will wear or fragment in very different ways ultimately.

CONCLUSIONS

It has been shown that environment definitely affects the measured frictional values for mineral/mineral, mineral/rock, or mineral/rock interfaces. The drier the surface, the higher the friction and this was true for all rock types tested. The increase in friction between atmospheric and UHV ranged from 2 to 3.6 for the sample types tested. The effect of temperature was positive in atmospheric pressure but negative in the UHV condition.

The mechanisms and extent of influence that the different environments and temperatures had on friction are complicated and are highly dependent on the material properties such as the fabric, porosity, and permeability.

Repeated traveling along the same track usually increased the friction regardless of testing environments. The increase tended to stabilize between the second and seventh run.

The junction theory of friction seems applicable to the friction between probe/mineral interfaces as evidenced by the numerous peaks and valleys occurring along the friction traces.

Since the Apollo missions seem to confirm the worst case condition, which was assumed in the original premise of this research, it appears that the experimental conditions nearly approximated those of the lunar surface. Drilling and other fragmentation techniques in the lunar environment may require changes in techniques due to the increased friction. This increase will be less in lunar day temperature for works involving friction of mineral on rock, or rock on rock, than in lunar ambient temperature condition, but larger for work with mineral/metal or rock/metal contact. This will be true for both surface and subsurface endeavors and will include fragmentation by drilling and other techniques.

RECOMMENDATIONS

Based on the results of this initial effort, several areas of friction in mineral/rock, metal/rock interfaces need further investigation. These include the mechanisms of friction and the effect of temperature. This work should be enlarged to include a study of static friction, sticking frequency, and magnitude of sticking and their relation to fragmentation and wear. The mechanisms of friction must be investigated by direct

correlation of friction traces with the microstructures of the specimen along the testing track. This could be assisted by videotaping through a microscope of the friction test to provide an enlarged view of the interface area. The temperature effect should be investigated by studying the chemical and physical changes in specimen surface which may alter the adhesive strength of the junction contacts as a result of temperature change. Before performing the friction tests, the physical properties of fabric, porosity, and permeability should be thoroughly investigated for the specimens being used.

Additional research is also needed to relate friction to fragmentation and wear in an applied manner. This effort should be extended to include loads between 5 and 35 pounds on the probe. This would then allow direct correlation of friction to drilling since exactly similar environments and sample handling techniques may be used with the UHV drill system. Such an approach in the laboratory to fragmentation, wear, and drilling would use controlled conditions to define the precise parameters needing field assistance.

Acknowledgments

We wish to express thanks to Kenneth G. Pung and James R. Blair for hours of work on the assembly and debugging of the electronics system used for data recovery, initial calibration of the total system, and assistance in performing experiments.

REFERENCES

1. Kragelskii, I. V. Friction and Wear. Translated from Russian by L. Ronson and J. R. Lancaster, Butterworth and Co., Limited, Washington, D.C., 1965, 346 pp.
2. Bowden, F. P., and D. Tabor. Friction and Lubrication. Methuen and Co., Ltd., London, 1967, 166 pp.
3. Horn, H. M., and D. U. Deere. Frictional Characteristics of Minerals. Geotechnique, v. 12, 1962, pp. 319-335.
4. Rae, D. The Measurement of the Coefficient of Friction of Some Rock During Continuous Rubbing. Journal of Scientific Instrumentation, v. 40, 1963, pp. 438-440.
5. Handin, J., and D. W. Stearns. Sliding Friction of Rock. Transactions of the American Geophysics Union, v. 45, 1964, 103 pp.
6. Brace, W. F., and J. D. Byerlee. Stick-slip as a Mechanism for Earthquake. Science, v. 153, No. 3739, Aug. 26, 1966, pp. 990-992.
7. Byerlee, J. D. Frictional Characteristics of Granite Under High Confining Pressure. Journal of Geophysical Research, v. 72, No. 14, July 15, 1967, pp. 3639-3648.
8. _____. Theory of Friction Based on Brittle Fracture. Journal of Applied Physics, v. 38, No. 7, June 1967, pp. 2928-2934.
9. Byerlee, J. D., and W. F. Brace. Stick-slip, Stable Sliding, and Earthquakes--Effect of Rock Type, Pressure, Strain Rate, and Stiffness. Journal of Geophysical Research, v. 73, No. 18, September 1968, pp. 6031-6037.

10. Hoskins, E. R., J. C. Jaeger, and K. J. Rosengren. A Medium Scale Direct Friction Experiment. *International Journal of Rock Mechanics and Mining Sciences*, v. 5, pp. 143-154.
11. Coulson, J. H. The Effects of Surface Roughness on the Shear Strength of Joints in Rock. Technical Report MRD 2-70, University of Illinois, Urbana, Ill., 1970, 282 pp.
12. Brace, W. F. Mechanics of Crustal Earthquakes. Final report, ARPA contract No. H0110376, monitored by U.S. Bureau of Mines, Twin Cities Mining Research Center, December 1971, 78 pp.
13. Weil, N. A. Lunar and Planetary Surface Conditions, *Advances in Space Science and Technology*. Supplement 2, Academic Press, 1965.
14. Green, J. Selection of Rock Standards for Lunar Research. *Annals New York Academy of Science*, v. 123, Art. 2, July 15, 1965, pp. 1123-1147.
15. Atchison, T. C., and C. W. Schultz. Bureau of Mines Research on Lunar Resource Utilization. Proceedings of the 6th Annual Meeting of the Working Group on Extraterrestrial Resources, Brooks Air Force Base, Texas, NASA SP-177, Feb. 19-21, 1968, pp. 65-74.
16. Fogelson, D. E. Simulated Lunar Rocks. Proceedings of the 6th Annual Meeting of the Working Group on Extraterrestrial Resources, Brooks Air Force Base, Texas, NASA SP-177, Feb. 19-21, 1968, pp. 75-95.
17. Roepke, W. W., and C. W. Schultz. Mass Spectrometer Studies of Outgassing From Simulated Lunar Materials in UHV. 14th National Symposium of the American Vacuum Society, October 1967, pp. 165-166.

18. Roepke, W. W. Friction Tests in Simulated Lunar Vacuum. Proceedings of the 7th Annual Meeting of the Working Group on Extraterrestrial Resources, Denver, Colo., NASA SP-229, June 1969, pp. 107-111.
19. Podlascek, S., and H. K. Shen. A Statistical Method for the Study of Friction and Wear in Vacuum, in Adhesion or Cold Welding of Materials in Space Environments. Pp. 272-314.
20. Atkins, J. O. Private communication on compressive strengths of rock in UHV.
21. Rabinowicz, E. Friction and Wear of Materials. John Wiley and Sons, Inc., 1965, 236 pp.

APPENDIX A

This appendix lists all the frictional values used for analysis of mineral probe/specimen interfaces measured under different environmental conditions. The test number in the first column of NT tests indicates the measurement number in each data set while those of ST tests indicates the number of repeated tests run on one track. Only those sets of data in NT tests which consist of more than 10 measurements are statistically analyzed and listed across the bottom of the appropriate tables.

TABLE 1. - Surface Friction in Probe/Specimen Interface Under Atmospheric Room Environment in New Track Tene

Test Number	Specimen Types										St. St.	St. St. (Pol.)
	Andesine	Besite	Diците	Feldspar (pk)	Feldspar (wh)	Labradorite	Magnetite	Pyroxene	Quartz	St. St.		
1	0.195	0.152	0.186	0.218	0.230	0.254	0.157	0.212	0.271	0.190	0.250	0.247
2	.192	.156	.211	.245	.226	.284	.171	.253	.240	.146	.259	.232
3	.194	.156	.182	.239	.230	.256	.180	.191	.262	.207	.245	.240
4	.214	.159	.203	.233	.212	.280	.165	.193	.268	.197	.246	.225
5	.174	.172	.193	.232	.235	.267	.194	.196	.209	.162	.239	.222
6	.197	.167	.208	.237	.225	.286	.184	.202	.267	.182	.246	.224
7	.211	.165	.193	.243	.236	.283	.176	.203	.263	.165	.244	.189
8	.197	.169	.210	.218	.220	.277	.191	.215	.257	.180	.256	.209
9	.228	.165	.187	.260	.240	.255	.181	.189	.271	.202	.252	.179
10	.163	.187	.207	.252	.221	.275	.214	.204	.259	.220	.269	.209
11					.215	.255			.223	.203		
12									.228	.197		
13									.241	.133		
14									.251	.2098		
15									.230	.207		
16									.247	.192		
17									.253	.2029		
18									.236	.1345		
19									.237	.2158		
20									.236	.2258		
21												
22												
Total	1.954	1.659	1.983	2.377	2.499	2.958	1.810	2.049	6.789	2.514	2.331	
Average	.197	.165	.198	.238	.227	.270	.181	.205	.229	.254	.214	
Min.	.153	.152	.182	.218	.212	.253	.157	.181	.133	.230	.169	
Max.	.228	.187	.211	.252	.240	.284	.214	.258	.271	.268	.247	
S.D.	.0128	.0128	.0111	.0134	.0095	.0161	.0161	.0212	.0159	.0096	.0255	
Var.	.00033	.00016	.00012	.00018	.00009	.00026	.00026	.00045	.00032	.00009	.00063	

TABLE 2. - Surface Friction in Probe/Specimen Interface
Under Atmospheric Hot Temperature
Environment in New Track Test

Test Number	Dacite	Specimen Types		St. St. (Pol.)
		Quartz	St. St.	
1	0.333	0.289	0.450	0.306

TABLE 3. - Surface Friction in Probe/Specimen Interface
Under Dry Nitrogen Room Temperature
Environment in New Track Test

Test Number	Basalt	Dacite	Specimen Types			St. St.	
			Labradorite	Magnetite	Pyroxene		
1	0.492	0.388	0.430	0.295	0.782	0.438	0.706
2	.528	.403	.405	.294	.766	.442	.723
Average	0.510	0.396	0.418	0.295	0.774	0.440	0.715

TABLE 4. - Surface Friction in Probe/Specimen Interface
Under Dry Nitrogen Hot Temperature
Environment in New Track Test

Test Number	Specimen Types		Labradorite
	Basalt	Dacite	
1	0.416	0.434	0.448
2	.379	.420	.435
3	.375		.425
4	.367		
Average	0.385	0.427	0.436

TABLE 5. - Surface Friction in Probe/Specimen Interface Under UHV
Room Temperature Environment in New Track Test

Test Number	Andesine	Beselt	Decite	Teldspar (pk)	Feldspar (wht)	Specimen Typas Labradorite	Magnetite	Pyroxene	Quartz	St. St.	St. St. (Pol.)
1	0.430	0.560	0.351	0.579	0.629	0.383	0.556	0.705	0.423	0.491	0.791
2	.438	.535	.427	.579	.750	.419	.421	.720	.360	.510	.992
3	.480	.595	.412	.553	.635	.443	.492	.715	.418	.492	.837
4	.485	.612	.487	.595	.582	.482	.306	.735	.342	.509	1.001
5	.500	.453	.448	.508	.546	.452	.385	.717	.410	.492	.803
6	.500	.565	.513	.575	.547	.608	.496	.703	.408	.520	.927
7	.502	.555	.603	.540	.542	.357	.422	.697	.406	.433	.873
8	.471	.552	.508	.543	.545	.465	.421	.712	.389	.492	1.012
9	.475	.506	.679	.513	.543	.450	.438	.712	.418	.521	.935
10	.478	.562	.520	.532	.561	.665	.362	.675	.396	.595	1.035
11		.532	.351	.498		.483	.415	.656	.308	.427	.696
12		.543	.391	.508		.408	.415	.656	.308	.427	.696
13		.538	.535	.508		.585	.384	.675	.378	.437	.702
14		.582	.521	.543		.472	.363	.662	.380	.412	.753
15		.530	.518	.538		.552	.315	.655	.381	.418	.718
16		.539	.468	.529		.470	.308	.665	.303	.410	.754
17		.523	.550	.528		.551	.303	.670	.363	.401	.770
18		.510	.462	.535		.493	.288	.640	.371	.416	.743
19		.500	.597	.539		.579	.282	.650	.350	.418	.767
20		.525	.542	.550		.498	.257	.652	.349	.412	.767
21		.514	.444			.729	.264				
22						.580					
23						.793					
24						.793					
25						.815					
26						.760					
27						.902					
28						.763					
29						.860					
30						.720					
31						.847					
32						.702					
Total	4.829	11.380	9.925	10.791	5.929	19.141	7.927	13.674	16.902	13.962	9.235
Average	.483	.542	.473	.540	.593	.593	.374	.684	.422	.698	.923
Min.	.458	.453	.351	.498	.542	.357	.257	.640	.308	.630	.791
Max.	.502	.612	.597	.595	.750	.902	.556	.735	.585	.770	1.042
S.D.	.0142	.0306	.0698	.0235	.0725	.0778	.0504	.0130	.0216	.0248	.0939
Var.	.00020	.00102	.0043	.00059	.0053	.0062	.00258	.00017	.00072	.0063	.00882

ORIGINAL SOURCE IS FILE

TABLE 6. - Surface Friction in Probe/Specimen Interface Under HV
 Not Temperature Environment in New Track Test

Test Number	Specimen Types										Quartz	St. St.	St. St. (Pol.)
	Andesite	Basalt	Dacite	Feldspar (pk)	Feldspar (wht)	Labradorite	Magnetite	Pyroxene	0.692	0.4125			
1	0.453	0.458	0.398	0.453	0.511	0.384	0.333	0.692	0.4125	0.779	1.430		
7	.455	.432	.430	.458	.527	.392	.328	.683	.378	.766	1.180		
3	.477	.438	.396	.467	.551	.404	.366	.707	.388	.772	1.240		
4	.438	.418	.474	.453	.567	.427	.366	.710	.3775	.763	1.195		
5	.466	.448	.424	.468	.538	.403	.331	.728	.378	.770	1.245		
6	.457	.458	.419	.469	.575	.395	.328	.730	.383	.773	1.255		
7	.469	.470	.402	.462	.627	.394	.348	.718	.4015	.758	1.290		
8	.468	.475	.409	.497	.655	.412	.328	.728	.428	.800	1.290		
9	.458	.422	.412	.476	.569	.393	.309	.730	.359	.785	1.260		
10	.464	.423	.409	.467	.618	.388	.312	.729	.382	.755	1.310		
11						.434			.483				
12						.428			.465				
13						.417			.413				
14						.436			.396				
15						.442			.412				
16						.446			.388				
17						.535			.398				
18						.457			.389				
19						.467			.404				
20						.470			.394				
21									.517				
22									.513				
23									.492				
24									.492				
25									.462				
26									.457				
27									.449				
28									.428				
29									.452				
30									.441				
Total	4.605	4.442	4.182	4.669	5.757	8.523	3.368	7.154	12.731	7.720	12.694		
Average	.461	.446	.418	.467	.576	.426	.337	.716	.424	.772	1.270		
Min.	.438	.418	.396	.453	.511	.384	.309	.683	.359	.755	1.180		
Max.	.477	.475	.474	.497	.655	.535	.386	.730	.517	.800	1.430		
S.D.	.0111	.0235	.0233	.0128	.0451	.0230	.0237	.0171	.0208	.0134	.0696		
Var.	.00012	.00042	.00054	.00017	.0020	.00063	.00056	.00029	.00070	.00018	.00484		

REPRODUCIBILITY OF THE ORIGINAL PAGE IS POOR

**TABLE 7. - Surface Friction in Probe/Specimen Interface
Under Dry Nitrogen Room Temperature
Environment in Same Track Test**

Test Number	Specimen Types			St. St.
	Dacite	Pyroxene	Quartz	
1	0.329	0.778	0.334	0.674
2	.335	.842	.343	.672
3	.380	.848	.368	.666
4	.398	.874	.395	
5	.436	.863	.431	
6	.472			

**TABLE 8. - Surface Friction in Probe/Specimen Interface Under UHV
Hot Temperature Environment in Same Track Test**

Test Number	Specimen Types	
	Dacite	Labradorite
1	0.420	0.425
2	.507	.508
3	.549	.629

REPRODUCTION OF
ORIGINAL DATA BY PEAR

TABLE 9. - Surface Friction in Probe/Specimen Interface Under UHV
Room Temperature Environment in Same Track Test

Test Number	Andesine	Bersalt	Dacite	Feldspar (pk)	Feldspar (wht)	Specimen Types				Quartz	St. St.	St. St. (Pol.)
						Labradorite	Magnetite	Pyroxene	Pyroxene			
1	0.579	0.490	0.412	0.574	0.523	0.498	0.711	0.538	0.754	1.256		
2	.704	.463	.441	.716	.676	.537	.723	.565	.744	1.220		
3	.728	.498	.509	.797	.704	.587	.747	.607	.751	1.213		
4	.734	.512	.578	.855	.718	.638	.749	.635	.754	1.195		
5	.723	.566	.633	.856	.730	.648	.742	.623	.727	1.140		
6	.756	.493	.676	.837	.747	.667	.757	.685	.717	1.164		
7	.787	.602	.686	.848	.745	.654	.768	.738	.707	1.085		
8	.771	.629	.716	.848	.740	.674	.772	.745	.672	1.080		
9	.728	.620	.742	.867	.768	.682	.793	.725	.704	.943		
10	.730	.642	.752	.869	.714	.682	.775	.754	.697	1.055		
11		.684	.759	.862			.803			1.007		
12		.795	.753				.808			.916		
13		.778					.825			.858		
14		.796					.807			.886		
15		.792					.818			.878		
16		.803										

